# Improving Soliton Transmission Systems Through Soliton Interactions

Gai Zhou, Tao Gui, Chao Lu, Alan Pak Tao Lau, and P.K.A. Wai

***Abstract*— Nonlinear interactions between neighboring pulses has always been a fundamental bottleneck in soliton transmission systems. Recently, coherent transceivers, digital signal processing (DSP) and the new nonlinear Fourier transform (NFT) theoretical framework has revived and generalized the field of soliton transmissions into nonlinear frequency division multiplexing (NFDM). We hereby demonstrate analytically and experimentally that one can considerably improve soliton transmission performance by intentionally allowing neighboring solitons to interact and collide during propagation and exchange positions at the receiver followed by standard NFT processing. This can be achieved by designing neighboring solitons' eigenvalues $\lambda$ to have opposite signs in the real part while the magnitude $|\Re(\lambda)|$ is optimized for a given transmission distance so that neighboring transmitted pulses would have swapped their timing positions at the receiver. Experimental results for 6.13 Gbaud 1-soliton systems demonstrate a transmission reach improvement of 100% for 16APSK and 60% for 8PSK modulated on the *b*-coefficients. The proposed scheme eliminated a long-standing fundamental limitation in soliton transmissions, opened up new dimensions in transmitter signal design and receiver signal processing for nonlinear optical communication systems.**

***Index Terms*—Optical communications, nonlinear Fourier transform.**

## I. Introduction

Soliton is one of the key research area in long-haul nonlinear fiber transmissions and has been studied for the past three decades [1, 2]. Characterizing and reducing impairments for transmission of fundamental solitons has been a central theme for telecommunication researchers and the wider nonlinear optics community. In long-haul soliton transmissions, periodic signal amplification with spontaneous emission noise results in soliton jitters known as Gordon-Haus effect [3-5], which is a long-standing problem in soliton transmissions. Additionally, in soliton systems where soliton pulse trains are generated and detected one pulse after the other, a linear superposition of two soliton pulses are in general not a solitonic solution to the Nonlinear Schrodinger Equation (NLSE) and hence neighboring pulses will interact with each other along propagation. The neighboring pulses will attract or repel from each other depending on their relative phase $\Delta\phi$ and such interactions are well documented in the literature [2, 6-9]. This will produce additional timing-jitters and push the pulses away from the preset detection time window which significantly degrades performance. On the other hand, when 2 wavelength-division multiplexing (WDM) solitons collide in time in the vicinity of an optical amplifier, the sudden change of the pulse energy creates asymmetric frequency shifts hence time shifts and additional jitters to pulses in neighboring channels [10]. The nonlinear interactions between neighboring pulses in time and/or neighboring WDM channels are therefore one of the most fundamental limitations in soliton transmissions. Consequently, a general design rule of thumb is that the pulse width needs to be about 1/5 of the pulse separation or symbol period [Chap. 9.2, 11] in order to suppress interactions and ensure reliable detection but in turn severely limit the spectral efficiency.

With coherent detection and digital signal processing (DSP) flourishing over the last decade, transmission capacities of optical fiber communication systems were tremendously improved. This is brought about by the ability to generate and detect arbitrary optical waveforms in two polarizations so that advanced high spectral efficiency modulation formats can be used. DSP also become powerful tools to combat transmission impairments such as chromatic dispersion (CD) and polarization-mode dispersion (PMD) and is highly adaptable. However, despite the success in mitigating linear impairments, fiber nonlinearity effects are still not effectively compensated through DSP. There has been a lot of attempts on this front such as digital back-propagation [12] but their performance improvements are only modest but their computational complexity inhibits its practical use.

Recently, the field of nonlinear Fourier transform (NFT) and nonlinear frequency division multiplexing (NFDM) has gained attention in the community. The NFT framework decomposes the NLSE into parallel channels and decomposes the signal into nonlinear spectral components, which can be obtained by solving the Zakharov-Shabat problem from the Lax pair operators corresponding to the NLSE. In this case, the NFT/inverse-NFT (INFT) operators transform the signal between time-domain and nonlinear frequency domain [13]. Hasegawa and Nyu first proposed to use the NFT concept for nonlinear fiber transmissions [14] in which information can be transmitted on the eigenvalues of the nonlinear channels without interfering each other. The concept is further combined with advances in digital coherent technology and generalized into NFDM [15-18]. NFDM is considered a generalized theoretical framework for nonlinear fiber transmissions in the sense that continuous spectrum resemble conventional orthogonal frequency division multiplexing

This work was supported by Hong Kong Government General Research Fund under project number PolyU 152116/15E.

Gai Zhou, Tao Gui and Alan Pak Tao Lau are with the Photonics Research Center, Department of Electrical Engineering, The Hong Kong Polytechnic University, Kowloon, Hong Kong. (e-mail: gai.zhou@connect.polyu.hk; tao.gui@connect.polyu.hk;alan.pt.lau@polyu.edu.hk).

Chao Lu and P.K.A. Wai are with the Photonics Research Center, Department of Electronic and Information Engineering, The Hong Kong Polytechnic University, Kowloon, Hong Kong. (e-mail: enluchao@polyu.edu.hk; alex.wai@polyu.edu.hk).

(OFDM) while discrete spectrum (eigenvalues) resemble solitons. Initial proof-of-concept experiments have demonstrated promising results [19-27]. Information-theoretic limits [28], DSP for NFT systems [25, 29-33] and advances in accurately and efficiently computing the NFT [34-36] and INFT operations [37, 38] are currently under intensive investigations.

The advent of digital coherent receivers and NFT framework give rise to new possibilities in solitons and general nonlinear signaling techniques for nonlinear fiber communication systems. The concept of coherent soliton communications was first proposed in [39] where 8PSK signals are considered and the perturbations to individual solitons and the overall pulse trains due to random phase difference between neighboring solitons are characterized. Timing jitters for phase modulated soliton systems are studied [3] and countermeasures such as digital backward propagation and in-line fixed frequency guiding filters were proposed [4, 5]. On the other hand, Frumin et al [33] proposed to encode information in multi-solitons to eliminate pulse interaction effects. In this paper, we took another direction of approach by intentionally design the neighboring solitons' eigenvalues λ to have opposite signs in the real part $\Re(\lambda)$ so that the solitons will strongly interact, collide and walk past each other irrespective of their initial relative phase $\Delta\phi$. We analytically show that the perturbations to the eigenvalue by neighboring pulses diminish with increasing $|\Re(\lambda)|$. Therefore, overall transmission performance can be significantly enhanced as long as $|\Re(\lambda)|$ is also chosen such that the original pulses are well separated and located within neighboring time slots for detection at the receiver. The proposed technique does not incur additional computational complexity compared to other single-soliton based NFT systems and are simpler than multi-soliton NFT/INFT. Experiments for 6.13 GBaud 8-phase-shift-keying (PSK) and 16-amplitude-phase-shift-keying (APSK) modulated 1-soliton pulses show that transmission reach can be extended by 60% and 100% respectively compared to recent phase and spectral magnitude modulated 1-soliton systems [23]. Our work highlights the *benefits* of pulse-to-pulse interactions in nonlinear transmission systems. The removal of the conventional soliton interaction constraint improves soliton transmission performance, provides new design parameters and opens up new directions for signaling and DSP research in communications over nonlinear fibers.

## II. Nonlinear Fourier Transform in Digital Coherent Systems

The equation governing signal propagation in fiber is the nonlinear Schrodinger Equation [40]:

$$j\frac{\partial}{\partial z}A(t,z)-\frac{\beta_2}{2}\frac{\partial^2}{\partial t^2}A(t,z)+\gamma|A(t,z)|^2A(t,z)=0 \tag{1}$$

where $A(t,z)$ is the signal, $t,z$ $\beta_2,\gamma$ are the physical time, distance, group-velocity dispersion (GVD) and fiber nonlinearity coefficient respectively. We can write the NLSE in a normalized form

$$j\frac{\partial}{\partial \ell}u(\tau,\ell)+sgn(\beta_2)\frac{\partial^2}{\partial \tau^2}u(\tau,\ell)+|u(\tau,\ell)|^2u(\tau,\ell)=0 \tag{2}$$

$$\ell=\frac{z}{L_D},\tau=\frac{t}{T_0},L_D=\frac{2T_0^2}{|\beta_2|},u=\sqrt{\gamma L_D}A \tag{3}$$

where $\tau,\ell,u$ are normalized time, distance and signal envelope respectively. Note that $T_0$ is a free normalization parameter. The NFT of a signal $u(\tau)$ (in normalized units), supported in the interval $\tau\in[T_1,T_2]$, is defined by solving the differential equation [1,16-18]

$$\frac{\partial v}{\partial \tau}=\begin{pmatrix}-j\lambda & u(\tau)\\ -u^*(\tau) & j\lambda\end{pmatrix} \tag{4}$$

$$v(T_1,\lambda)=\begin{pmatrix}v_1(T_1,\lambda)\\ v_2(T_1,\lambda)\end{pmatrix}=\begin{pmatrix}1\\0\end{pmatrix}exp(-j\lambda T_1) \tag{5}$$

where $\lambda$ and $v(\tau,\lambda)$ are, respectively, the eigenvalue and eigenvector. Defining the *a*-coefficient and *b*-coefficient as

$$a(\lambda)=v_1(T_2,\lambda)\,exp(j\lambda T_2)$$
$$b(\lambda)=v_2(T_2,\lambda)\,exp(-j\lambda T_2)$$

The nonlinear spectrum of $u(\tau)$ is made of a continuous and a discrete spectrum. The continuous spectrum is defined as $q_c(\lambda)=b(\lambda)/a(\lambda)$ for $\lambda\in\mathbb{R}$. The discrete spectrum is defined as $q_d(\lambda)=b(\lambda)/a'(\lambda)$ (where $a'(\lambda)=da(\lambda)/d\lambda$) at isolated roots $a(\lambda)=0$ in the upper-half complex plane $\lambda\in\mathbb{C}^+$. During signal propagation, the nonlinear spectrum evolves with distance as

$$q_c(\lambda,\ell)=q_c(\lambda,0)exp(4j\lambda^2\ell)$$
$$q_d(\lambda,\ell)=q_d(\lambda,0)exp(4j\lambda^2\ell) \tag{6}$$

with $\ell$ being the normalized distance. In analogy with linear systems, nonlinear frequency division multiplexing (NFDM) suggests that independent information should be encoded on different parts of the nonlinear spectra so that they will all propagate along the fiber without mutual interference. With coherent detection and digital signal processing (DSP) in this current generation of transceiver technology, the NFDM concepts can now be experimentally implemented. The process of converting the nonlinear spectrum into time-domain waveform is the INFT.

Waveforms with only discrete spectrum are known as solitons. The simplest soliton contains only 1 eigenvalue $\lambda\in\mathbb{C}^+$ with discrete spectrum $q_d(\lambda)$ and is given by

$$u(\tau)=-2j\Im(\lambda)\,sech\big(2\Im(\lambda)(\tau-\tau_0)\big)\times exp\big(-2j\Re(\lambda)\tau-j\angle q_d(\lambda)\big)$$

where

$$\tau_0=\frac{1}{2\Im(\lambda)}ln\frac{|q_d(\lambda)|}{2\Im(\lambda)}$$

In this case, the physical interpretations of the spectral parameters are straight forward. $\Im(\lambda)$ determines the peak amplitude and width of the soliton while $\Re(\lambda)$ determines center frequency shift, which in turn determines the soliton's group velocity. $|q_d(\lambda)|$ and $\Im(\lambda)$ together determine the soliton's initial position $\tau_0$ while the soliton's phase is given by $\angle q_d(\lambda)$.

In terms of DSP techniques, we recently showed [25] that for discrete eigenvalue transmissions with phase and magnitude modulation of $q_d(\lambda)=b(\lambda)/a'(\lambda)$, it is the *b*-coefficient $b(\lambda)$ that is modulated and undergoes $b(\lambda,\ell)=b(\lambda,0)e^{4j\lambda^2\ell}$ while $a'(\lambda)$ does not carry information and only contain noise. Therefore, $b(\lambda)$ can be used as a decision statistic instead of $q_d(\lambda)$. Furthermore, as distortions on $b(\lambda)$ due to amplifier noise are found to be correlated with distortions on λ and $a'(\lambda)$ [17], a simple linear minimum mean square error (LMMSE) filter that exploits such noise correlations is shown to considerably improve detection

performance.

## III. Pulse Overlapping and Soliton Interactions

An ideal NFDM system requires one to generate and detect the whole waveform. However, as the processing complexity and latency [41-43] increase with the energy and duration of the waveform, it is more desirable for practical INFT/NFT algorithms to generate and process multiple shorter waveforms with separated non-overlapping time windows. Since the NFT/INFT operators are not linear operators, even if waveforms $u_1(\tau)$ and $u_2(\tau)$ are well-separated in time, the sum

$$NFT\big(u_1(\tau)+u_2(\tau)\big) \neq NFT\big(u_1(\tau)\big)+NFT\big(u_2(\tau)\big) \quad (7)$$

and it is inevitable that each individual waveform will be perturbed by neighbors.

In case of soliton transmission as depicted in Fig. 1, soliton pulses are generated and processed in time-window $\tau \in [-T/2, T/2]$, where $T$ is normalized time-window width. We are going to prove although the eigenvalues and spectral amplitudes of each soliton will only be slightly perturbed by overlapping in the beginning, the distortions will accumulate with propagation distance and will become significant transmission impairments for long-haul links.

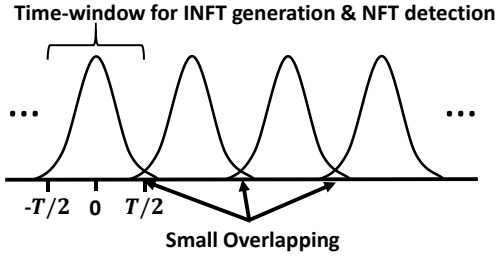


Fig. 1. Practical soliton pulse train are generated and detected one pulse after the other in separated time windows $\tau \in [-T/2, T/2]$, where $T$ is normalized time-window width. When the pulses are put together, they will overlap with each other and create distortions to the eigenvalues and spectral amplitudes of neighboring solitons

The perturbations from overlapping soliton pulses are well-understood [6-9], including the perturbation theory on $\lambda$ [6, section. 3]. Assume the pulse $u_0$ is perturbed by overlapping with a small value $\Delta u$ so that

$$u(\tau) = u_0(\tau) + \Delta u(\tau), \quad (8)$$

the first order perturbation on the eigenvalue $\lambda_n$ of $u_0$ can be written as:

$$\Delta\lambda_n = -\frac{j\int_{-\infty}^{\infty} v_n^T(\tau,\lambda_n)\sigma_2 \Delta U v_n(\tau,\lambda_n)d\tau}{\int_{-\infty}^{\infty} v_n^T(\tau,\lambda_n)\sigma_3\sigma_2 v_n(\tau,\lambda_n)d\tau} \quad (9)$$

$$\Delta U = \begin{pmatrix} 0 & \Delta u(\tau) \\ \Delta u^*(\tau) & 0 \end{pmatrix}, \sigma_2 = \begin{pmatrix} 0 & -j \\ j & 0 \end{pmatrix}, \sigma_3 = \begin{pmatrix} 1 & 0 \\ 0 & -1 \end{pmatrix} \quad (10)$$

where $v_n$ is the eigenvector of $\lambda_n$. According to [1, section. 5], when we assume two well-separated 1-soliton pulses with time separation $2\tau_0$ and phase difference $\Delta\phi$ given by

$$u(\tau) = sech(\tau-\tau_0) + exp(j\Delta\phi)\, sech(\tau+\tau_0), \quad (11)$$

the expression for the eigenvalue perturbation will be

$$\Delta\lambda = -\frac{sin(\Delta\phi)\,[1-2\tau_0\, coth(2\tau_0)]}{sinh(2\tau_0)} + j\frac{2\,cos(\Delta\phi)\,\tau_0}{sinh(2\tau_0)} \pm \frac{sin\left(\frac{\Delta\phi}{2}\right)\left[1-\frac{2\tau_0}{sinh(2\tau_0)}\right]}{2\,sinh(\tau_0)} \pm j\frac{cos\left(\frac{\Delta\phi}{2}\right)\left[1+\frac{2\tau_0}{sinh(2\tau_0)}\right]}{2\,cosh(\tau_0)} \quad (12)$$

Perturbations on the $\Re(\lambda)$ and $\Im(\lambda)$ depends on the phase difference $\Delta\phi$. For two neighboring 1-solitons with $\Delta\phi = 0$, only $\Im(\lambda)$ will be perturbated. On the other hand, $\Delta\phi \neq 0$ will induce $\Re(\lambda)$ perturbation on the two solitons and they will no longer be bounded in time and can move away/towards each other. Since information can now be encoded in the phase $\Delta\phi$ and magnitude of the spectral amplitude with digital coherent transceivers, such perturbations will also become random and pattern dependent. The consequences are: 1) the $b$-coefficient after propagation is given by

$$b(\lambda+\Delta\lambda,\ell) = b(\lambda+\Delta\lambda,0)\, exp(4j(\lambda+\Delta\lambda)^2\ell) \approx b(\lambda+\Delta\lambda,0)\, exp(4j(\lambda^2+2\lambda\Delta\lambda)\ell) \quad (13)$$

so that the distortions in the $b$-coefficient after equalization grows with distance through

$$exp(4j(\lambda+\Delta\lambda)^2\ell)\cdot exp(-4j\lambda^2\ell) \approx exp(8j\lambda\Delta\lambda\ell) \quad (14)$$

and 2) perturbations in $\Delta\lambda$ can distort the timing positions and produce jitters so that the soliton may walk out of the pre-set detection time window and significantly degrade performance. An example for the received noise variance $\sigma_b^2$ of $b$-encoded 8PSK signals as a function of normalized distance is shown in Fig. 2. The eigenvalue of the signals is $\lambda = 1j$. Solitons are in the center of time-window by setting $|q_d(\lambda)| = 2\Im(\lambda)$. The normalized time-window length is set to be 3.9 which contains 99.9% of the pulse energy. The parameters correspond to simulation of 6 GBaud (physical time window of around 167ps ) 8PSK transmissions in lossless and noiseless Non-Zero Dispersion-Shifted Fiber (NZDSF) with dispersion coefficient $D \cong 4$ ps/nm-km, normalized parameter $T_0 = 42.7\ ps$ and hence normalized distance $\ell = 1$ equals 357.9 km. In the simulation, the received $b$-coefficients are obtained by performing NFT for each time-window. While the 2-pulse model in Eq. (11) may not be accurate analysis of $\Delta\lambda$ and their effects for general pulse trains, it is obvious from Fig. 2 that the initial random $\Delta\lambda$ induce ever-growing distortions on the $b$-coefficients with propagation distance, a trend that aligns with the insights from Eq. (8) to Eq. (14).

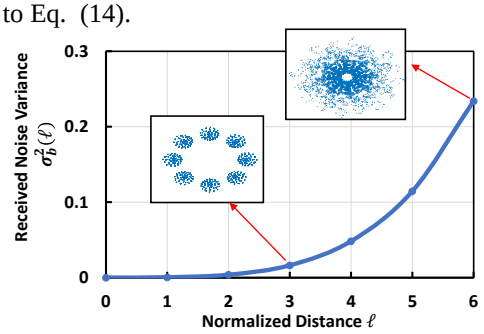


Fig. 2. Variance of received $b$-coefficients as a function of normalized propagation distance for an ideal lossless and noiseless fiber channel. The time window contains 99.9% of the pulse energy. Even though the eigenvalue distortions $\Delta\lambda$ maybe small at the transmitter, the distortions accumulate and significantly worsen performance as distance increases.

When we increase the baud rate, duration for each physical time-window decrease, which in turn reduce the normalized parameter $T_0$ and increases the normalized distance for a given physical distance. To reduce pulse overlapping, one can shortening the pulse time-duration. For soliton pulses, time-duration can be shortened by increasing $\Im(\lambda)$ but suffers from more noise because the signal bandwidth is increased [17, 44].

Increasing the time separation between the solitons will reduce overlapping but in the expense of reduced transmission capacity. Consequently, soliton interactions are a bottleneck for high speed soliton communications.

## IV. Interaction-tolerant Soliton Transmissions

Following [6, section. 5], the eigenvector of a 1-soliton located at $\tau = \tau_0$ with eigenvalue $\lambda = \alpha + \beta j$ and $\angle q_d(\lambda) = \phi$ can be written as

$$v = \begin{pmatrix} v_1 \\ v_2 \end{pmatrix} = \frac{1}{2} sech[\,2\beta(\tau - \tau_0)] \times \begin{pmatrix} \exp(-\beta(\tau - 2\tau_0) - j\alpha\tau) \\ -j\exp(\beta\tau + j\alpha\tau + j\phi) \end{pmatrix} \quad (15)$$

Now, consider a train of solitons with eigenvalues $\lambda = \pm\alpha + 1j$ and separated by $2\tau_0$ as shown in Fig. 5 (a). For simplicity, let us just analyze the interactions between pulse 1 and 2 so that the overall signal is given by $u(\tau) = u_1(\tau) + u_2(\tau)$ where

$$u_1(\tau) = 2\,sech\big(2(\tau + \tau_0)\big)\,exp(-2j\alpha\tau) \quad (16a)$$

$$u_2(\tau) = 2\,sech\big(2(\tau - \tau_0)\big)\,exp(2j\alpha\tau - j\Delta\phi) \quad (16b)$$

Let pulse 1 (Eq. (16a)) be the pulse of interest so that pulse 2 (Eq. (16b)) is the perturbation $\Delta u = u_2$. Substituting the corresponding eigenvector $v$ into Eq. (9) results in Eq. (17). Note that the integrand in Eq. (17) contain a pulse-like term $sech^2(2\tau')\,sech\big(2(\tau' - 2\tau_0)\big)$ and complex exponential terms

$$g(\alpha, \Delta\phi, \tau') = exp(-2(1 - j\alpha)\tau')\,exp(-2j\alpha\tau_0 - j\phi) + exp(2(1 - j\alpha)\tau')\,exp(2j\alpha\tau_0 + j\phi)$$

Fig. 3 plots these terms with different values of $\alpha$ for $\tau_0 = 1.95$. One can deduce that when $\alpha$ is small, the total area i.e. $\Delta\lambda$ depends on $\Delta\phi$. However, as $\alpha$ increases, the rapidly-varying sinusoid of $g(\alpha, \Delta\phi, \tau')$ will balance out the positive and negative areas of the integrand in Eq. (17) so that $\Delta\lambda \to 0$ irrespective of the relative phase $\Delta\phi$. Fig. 4 (a) shows the $\Delta\lambda$ obtained from Eq. (17) and compared with the $\Delta\lambda$ obtained from the NFT of the composite 2-pulse waveform $u(\tau) = u_1(\tau) + u_2(\tau)$, which is a 2-soliton. In this case, the eigenvalue distortion $\Delta\lambda$ stems from the fact that $u_1(\tau)$ and $u_2(\tau)$ are separate 1-solitons while the eigenvalues of their sum are not exactly $\pm\alpha + 1j$ but slightly distorted. It can be seen that $\Delta\lambda$ are similar for both cases and most importantly, $\Delta\lambda$ clearly diminish with increasing $\alpha$. The 2-pulse NFT preserves the eigenvalue upon transmission under ideal NLSE which allow us to approximate map the $\Delta\lambda$ of the transmitted waveform and its analysis to the received waveform. Fig. 4 (b) shows the variance of $\Delta\lambda$ for a 6 Gbaud pulse trains of 8PSK modulated on *b*-coefficient for back-to-back and 2147 km transmission of ideal lossless fiber without noise and show how the variance of $\Delta\lambda$ decreases with increasing $\alpha$ (the choice of $\alpha$ for 2147 km transmission will be described later in this section). Therefore, increasing $\alpha$ can help eliminate the

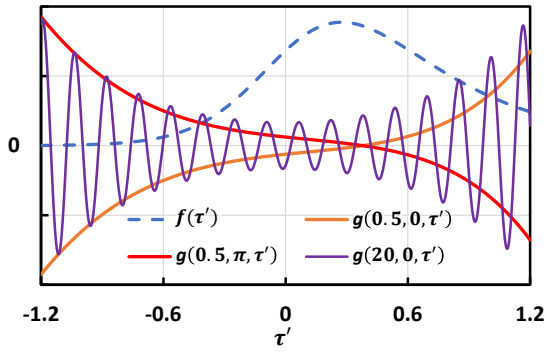


Fig. 3. The terms $f(\tau')$ and $g(\alpha, \Delta\phi, \tau')$ in Eq. (17). As $\alpha$ increases, the rapidly-varying sinusoid of $g(\alpha, \Delta\phi, \tau')$ will balance out the positive and negative areas of the product $f(\tau') \cdot g(\alpha, \Delta\phi, \tau')$ so that the total area under hence $\Delta\lambda$ will approach 0 irrespective to the phase difference $\Delta\phi$ between neighboring pulses.

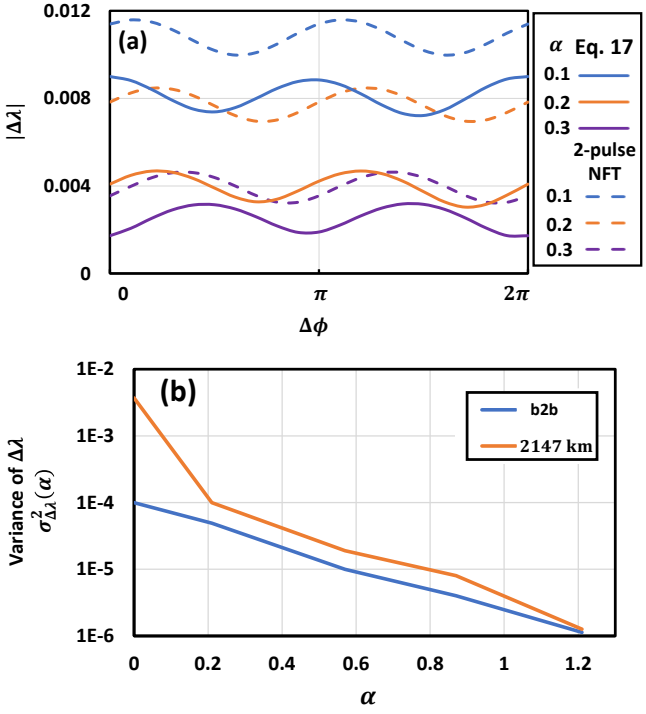


Fig. 4. (a) Eigenvalue distortions $\Delta\lambda$ due to neighboring solitons using perturbation theory and NFT of the composite 2-pulse waveform $u(\tau)$, illustrating that $\Delta\lambda$ decreases with increasing $\alpha$. (b) Variance of $\Delta\lambda$ vs. $\alpha$ for 6 Gbaud 8PSK transmissions for back-to-back and over 2147 km ($\ell = 6$) of ideal lossless fiber without noise.

$$\Delta\lambda = -\frac{\int_{-\infty}^{\infty}\big(\Delta u^*(\tau)v_1^2(\tau,\lambda) - \Delta u(\tau)v_2^2(\tau,\lambda)\big)d\tau}{2\int_{-\infty}^{\infty} v_1(\tau,\lambda)v_2(\tau,\lambda)d\tau}$$

$$= \frac{\int_{-\infty}^{\infty} sech^2\big(2(\tau+\tau_0)\big)\,sech\big(2(\tau-\tau_0)\big)\,(exp(-[2(\tau+\tau_0) - 2j\alpha\tau] - j\phi) + exp([2(\tau+\tau_0) - 2j\alpha\tau] + j\phi))d\tau}{\int_{-\infty}^{\infty} sech^2\big(2(\tau-\tau_0)\big)\,d\tau}$$

$$= \int_{-\infty}^{\infty} \underbrace{sech^2(2\tau')\,sech\big(2(\tau'-2\tau_0)\big)}_{f(\tau')} \underbrace{(exp(-2(1-j\alpha)\tau')\,exp(-2j\alpha\tau_0 - j\phi) + exp(2(1-j\alpha)\tau')\,exp(2j\alpha\tau_0 + j\phi))}_{g(\alpha,\Delta\phi,\tau')}\,d\tau' \quad (17)$$

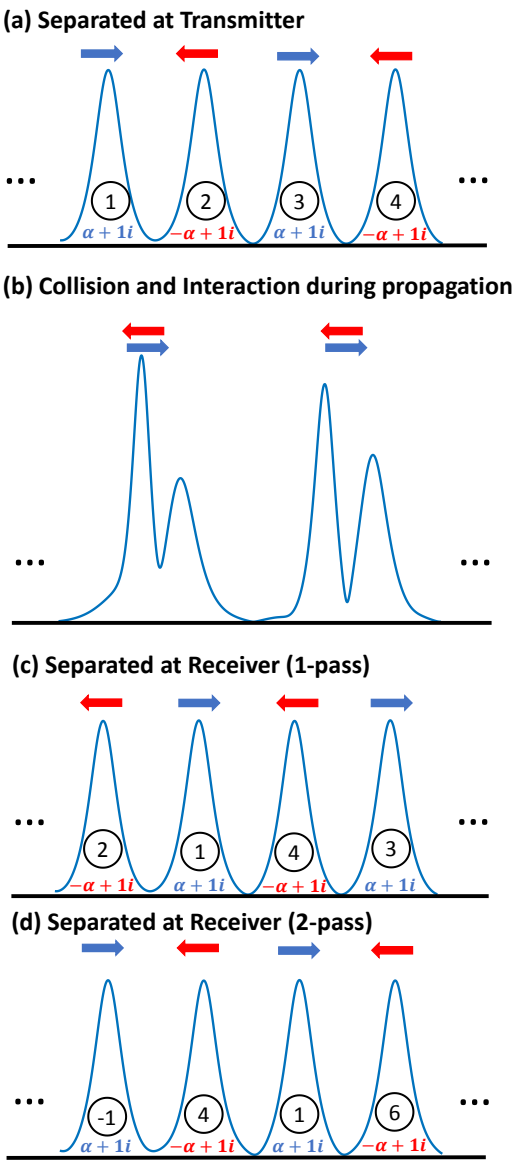


Fig. 5. Proposed interaction-tolerant discrete-eigenvalue transmissions using neighboring pulses with alternating eigenvalues' real part at the transmitter. Simulated transmissions of 6 Gbaud pulse trains with (b) α = 0.21 and $z$ = 1073 km; (c) α = 0.21 and $z$ = 2147 km (1-pass); (d) α = 0.57 and $z$ = 2147 km (2-pass). The number in circles are sequence numbers of the respective solitons in the pulse train. The solitons will walk off and interact with multiple neighboring pulses during propagation. But by appropriate design of $\alpha$ for a given transmission distance, the pulses can be well-separated at the receiver for detection.

random interactions and eigenvalue perturbations due to the relative phase between neighboring solitons, which in turn reduce the noise in the $b$-coefficient through Eq. (14), reduce timing jitters and thus improve transmission performance.

However, as $\alpha$ is closely related to the physical frequency hence group velocity of the pulse, increasing $\alpha$ will exemplify pulse walking off their pre-set detection time window, collide, strongly interact and degrade detection performance. Instead of suppressing the interactions and ensuring the solitons are well-located within their own detection time-windows, we hereby propose an interaction- tolerant signaling scheme in which neighboring pulses have eigenvalues with alternating real parts $\pm\alpha$ so that they every pair of transmitted pulse will walk towards each other and interact strongly. However, for a given distance $\ell$ (or real distance $z$), we choose $\alpha$ accordingly so that a given transmitted pulse is well-located in the time window of neighboring pulses at the receiver. This can be graphically interpreted as letting the pulse walk past each other during transmission and essentially swapping positions at the receiver as shown in Fig. 5. In this case, the benefit of large $\alpha$ while ensuring the received pulses can be individually detected in neighboring time windows of the same duration is that no additional computational complexity is incurred compared to standard 1-soliton systems and the baud rate is not compromised due to pulse walk-offs.

In the proposed setup, the solitons with odd sequence number have $\Re(\lambda) = \alpha$ while even sequence have $\Re(\lambda) = -\alpha$ at the transmitter. In the figure, the arrows represent the walk off direction of solitons during propagation. The variation of solitons during propagation is obtained from numerical simulation of 6 Gbaud 8PSK signal modulated on $b$-coefficient with $\lambda = \pm\alpha + 1i$ and $T = 3.9$. Solitons with odd and even sequence number will interact with each other as shown in Fig. 5 (b) and then move away from each other. The speed of solitons depends on α which is chosen to ensure the received solitons are centered at detection time windows of neighboring pulses as shown in Fig. 5 (c, d). In this case, the detection time windows are the same as conventional soliton or more general NFT systems. Furthermore, one can build on this concept and allow each soliton pulse to pass through multiple pulses during propagation before it is well-separated and located at the receiver. Let us denote a system in which each soliton walks off and passes $N_p$ neighboring solitons during transmission as an $N_p$-pass system. In this case, $N_p$ also represents the total number of collisions for each soliton. The value $\alpha$ is related to the transmission distance $\ell$, $\Im(\lambda)$ and $N_p$ but not exactly a linear function of $N_p$ and $\ell$ because the individual solitons and its speed during collisions is not constant or even well-defined [10]. The optimized value of α for 1-pass and 2-pass in Fig. 5 (c, d) are respectively 0.21 and 0.57 with z = 2147 km ($\ell = 6$). Therefore, in the following simulations and experiments, the best $\alpha$ is numerically estimated beforehand by numerical studies of pulse propagation before simulating transmission performance.

We conducted simulations of 6 GBaud 8PSK modulated soliton pulse train transmissions over 2147 km ($\ell = 6$) with different pass-through numbers $N_p$ in NZDSF fiber with physical time window around 167ps, corresponding to a normalized time window of T = 3.9. The eigenvalue is chosen to be $\Im(\lambda) = 1$ with $|q_d(\lambda)| = 2\Im(\lambda)$ and $|b(\lambda)| = 1$ so that the solitons are in the center of their respective time windows [45, 46]. We numerically estimate $\alpha \approx 0, 0.21, 0.57, 0.87, 1.21$ for $N_p = 0,1,2,3,4$. The noise variance on $\Delta\lambda$ for of ideal lossless fiber propagation without noise is shown in Fig. 4(b) and the noise variance of the received $b$-coefficient is shown in Fig. 6 for different fiber propagation models. We first transmit the pulse trains in an ideal lossless and noiseless NLSE channel and lossless and noisy channel. This is followed by simulating a multi-span link with span length 50 km in which signal loss for a fiber with attenuation 0.2 dB/km is compensated by an inline optical amplifier with 5 dB Noise figure for the noisy setup and no noise for the noiseless setup.

It should be noted that in principle, the signal launched power is determined by $\Im\{\lambda\}$ [16]. In practice, the signal power that optimize transmission performance (given a particular $\Im\{\lambda\}$) will deviate from the theoretical value due to fiber loss and other practical constraints. Typically, the optimal signal power for realistic systems with fiber loss will be higher than that from theoretical calculations assuming an ideal lossless fiber model. This can be intuitively understood by noting that higher power is needed to roughly offset the fiber loss so that the balance between fiber nonlinearity and chromatic dispersion is maintained for soliton transmissions. Consequently, for each $N_p$, the lossy cases in Fig. 6 are re-optimized over signal launched powers. It is interesting to note that the overall performance of noisy-lossy case is better than noisy-lossless, which may look counter-intuitive at the first glance. While fiber loss breaks the integrability of the NLSE and creates additional distortions to $\Delta\lambda$, the amount of nonlinear effects weakens along propagation in principle due to signal loss. Furthermore, as the optimized signal power for lossy case is higher than the corresponding lossless case, the OSNR is also higher in principle. Therefore, the overall performance in presence of loss is not guaranteed to be worse than lossless scenarios and it certainly is interesting to investigate this phenomenon more analytically as future research. Nonetheless, it is clear that the distortions on the received $b$-coefficients are significantly reduced when one allows the pulses to collide and interact during propagation by increasing $\alpha$ irrespective to the fiber propagation model. Nonetheless, for the lossy models, the noise variance exhibits a slight rebound after $N_p = 3$.

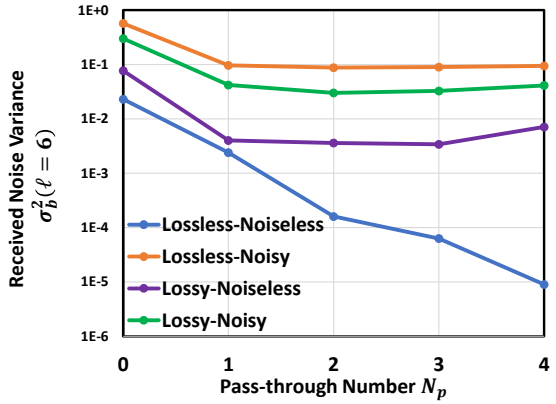


Fig. 6. Received noise variance of 6 GBaud 8PSK signals modulated on $b$-coefficient transmitted over 2147 km ($\ell = 6$) for different fiber propagation models. The distortions on $b$-coefficient decreases significantly when $N_p$ increases.

## V. Experimental Investigations

### A. Experiment Setup

We also conducted an offline experiment to further verify the proposed interaction-tolerant pulse-train scheme. Fig. 7 shows the experimental setup and offline DSP structure. At the transmitter side, random symbols were mapped onto the discrete spectrum for generated soliton pulse trains by inverse NFT. Here, 2 modulation formats, 8PSK and 16APSK were respectively tested for comparison in the experiments. The constellation shapes are shown in Fig. 7. The radius of 8PSK constellation is set as $|b(\lambda)| = 1$ with $|q_d(\lambda)| = 2\Im(\lambda)$ so that the solitons are symmetric and hence located at the center of their respective time-windows. Such constellation designs apply to different values of $\alpha$ in our study. Similar to [23], the distance $d$ between the 2 rings of the 16APSK were respectively optimized for each pass-through number as $d$ determines the pulse shift with respect to the given time interval.

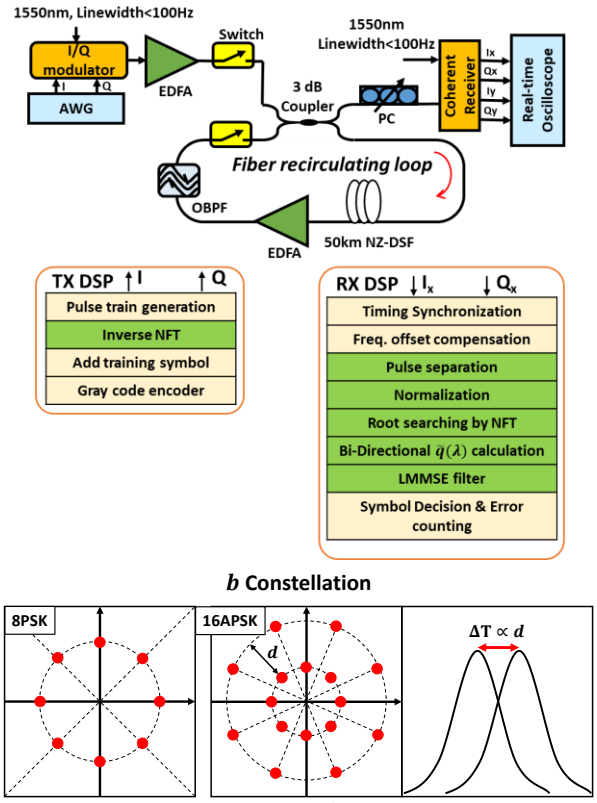


Fig. 7. Experimental Setup and modulation formats investigated.

Pre-adaptation as [47] was employed to pre-compensate the imperfection of transmitter components then sent to an arbitrary waveform generator (AWG) with 92 GSa/s to generate the electrical waveform of the pulse-train. The signal baudrate is 6.13 GBaud with 15 samples per pulse. Physical time-duration for each pulse is around 163 ps, corresponding to a normalized time window of 3.9 and normalization parameter $T_0 = 41.8\,ps$ from Eq. (3). The total bit rate of the designed system is 18.4 Gbps with 8PSK and 24.5 Gbps with 16APSK. After conversion by the I/Q modulator, the optical waveform was amplified and launched into fiber-loop. The loop consists of 1 span 50-km NZDSF and lumped amplification only by EDFA. A flat-top optical filter with a 3-dB bandwidth of 1 nm was used inside the loop to suppress the out-of-band amplified spontaneous emission (ASE) noise. Both the transmitter laser and local oscillator were from fiber laser sources with very low laser phase noise (NKT Koheras ADJUSTIK Fiber laser with linewidth < 100Hz). After alignment by a polarization controller in the x-polarization, the received signal was then coherently detected and sampled by a digital storage scope with a sampling rate of 80 GSa/s and a bandwidth of 33 GHz. The sampled signal was analyzed by off-line digital signal processing (DSP), whose structure is also shown in Fig. 7. After timing synchronization and frequency

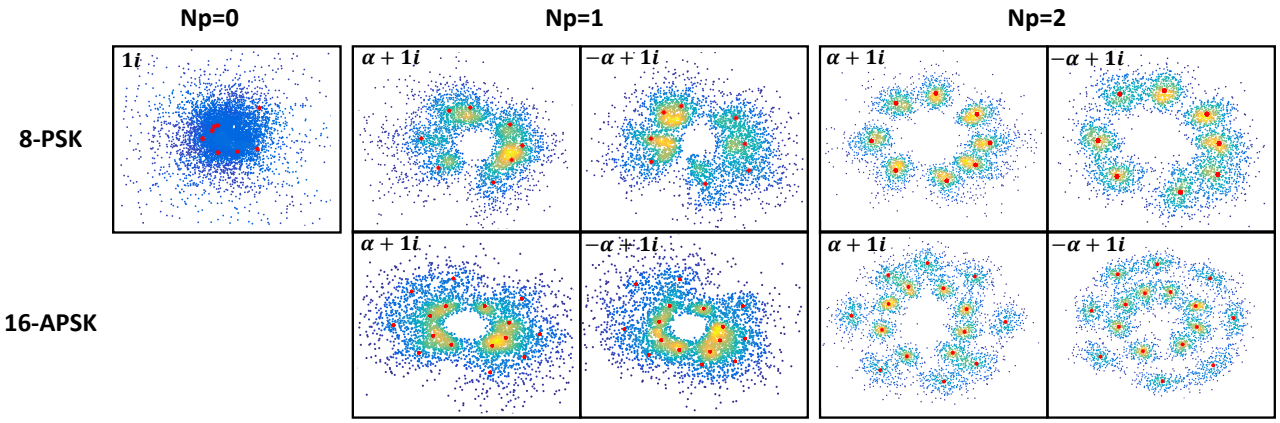


Fig. 8. Received $b$-coefficient distributions for 8PSK and 16APSK signals transmitted over 1500 km with optimized launch power. In case of $N_p$ = 1,2, distributions of two eigenvalues $\{\alpha+1i, -\alpha+1i\}$ are shown separately. Red dots are the mean of each received symbol. The received magnitude $|b|$ is processed and detected in log scale.

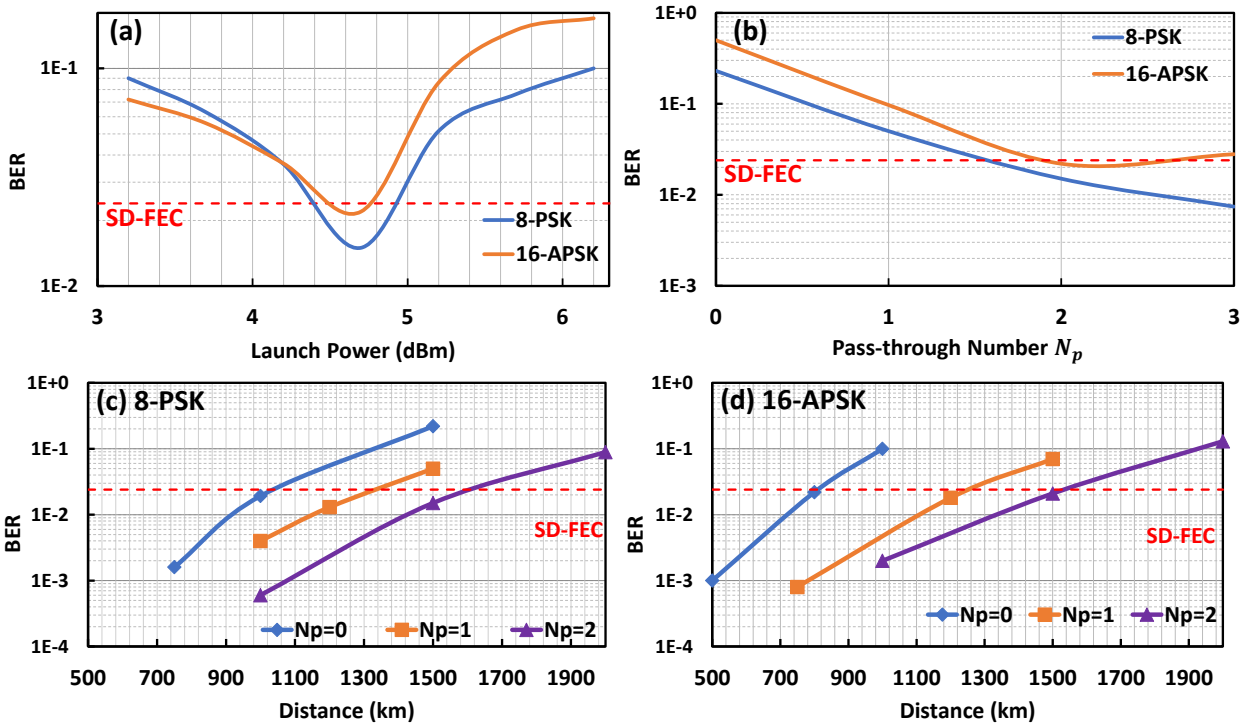


Fig. 9. (a) BER versus launch power for transmission over 1500 km for $N_p$=2. The optimal launch power for both modulation format is similar; (b) BER versus pass-through number $N_p$ for 8PSK/16APSK transmission over1500 km. The BER for each $N_p$ are optimized over signal launched power; BER vs. propagation distance for (c) 8PSK and (d) 16APSK signals with $N_p$ = 0,1,2. For slightly over 1500 km transmissions, the BER performance can achieve below SD-FEC threshold when $N_p$ = 2, while conventional soliton pulse trains ($N_p$ = 0) can only meet the SD-FEC threshold when the distance is reduced to 1000 km and 780 km for 8PSK and 16APSK signals respectively.

offset compensation, the received signal for both static and relative-approach pulse-train were separated into blocks for further NFT processing to recover the nonlinear spectrum. The last steps were symbol decision and bit error rate (BER) calculations. LMMSE filter [25] was adopted to compensate the noise of the $b$-coefficients via the correlation between the noise on $b$-coefficients and the roots.

*B. Experimental Results*

Both 8PSK and 16APSK modulation formats are investigated in experiments and their constellations are shown in Fig. 7. For 16APSK, the separation $d$ between the two constellation rings are numerically optimized for each pass-through number $N_p$. The value of $\alpha$ is numerically determined for each transmission distance and $N_p$ through simulations. To improve the detection performance, the LMMSE is always applied to the received $b$-coefficients. The received signal distributions of the LMMSE filter outputs are shown in Fig. 8 with different $N_p$ and slight distortions to the signal constellations can be seen. To alleviate the influence from such distortions, we re-calibrate the mean of each symbol class (red dots in Fig. 8) from training symbols and use minimum Euclidean distance based detection. It should be noted that we

detect the magnitude of the received $|b|$ in log scale.

We performed a sweep of signal launched power after the inverse NFT and the BER performance are depicted in Fig. 9 for different signal launched powers, transmission distances and $N_p$. Again, the signal power that optimize transmission performance (given a particular $\Im\{\lambda\}$) will deviate from the theoretical value due to fiber loss and other practical constraints. Fig. 9 (a) shows that best launch power for 1500 km transmission with $N_p$ = 2 is around 4.7 dBm for both modulation formats while the theoretical signal power is around 4.1 dBm. With the BER corresponding to the best launched power for each $N_p$, Fig. 9 (b) shows the optimized BER for different $N_p$ for both modulation formats. The performance improvements from our proposed interaction-tolerant soliton transmission design is clearly illustrated and agree with theoretical predictions as the BER decreases with increasing $N_p$. Nonetheless, it can be seen from Fig. 9 (b) that the benefits of intentional pulse-to-pulse interactions start to diminish when $N_p$ increases beyond 3, in agreement with simulation results for the lossy cases. This may be attributed to fiber loss as depicted in Fig. 6 as well as other component imperfections in the experimental setup. Fig. 9 (c, d) depicts the BER vs distance for both formats. For the soft-decision forward error correction (SD-FEC) threshold of 2.4E-2 (assuming an inner LDPC code with rate 9/10 and an outer hard-decision (HD)-FEC staircase code with 6.25% overhead [48]), transmissions over 1600 km and 1540 km can be achieved with $N_p = 2$ for 8PSK and 16APSK formats respectively while for conventional soliton pulse trains with $\alpha = 0$, the SD-FEC threshold can only be met at a reduced distance of 1000 km for 8PSK and 780 km for 16APSK formats. Therefore, the proposed interaction-tolerant soliton transmission technique results in a reach improvement of around 60% and 100% for 8PSK and16APSK signals respectively. It should be noted that joint statistical processing of multiple neighboring pulses and performing the NFT on them as multi-soliton waveforms can potentially give further performance improvements and these are interesting topics for further research.

Finally, Fig. 10 shows the back-to-back and received physical spectrum for 6.13 Gbaud 8PSK signals transmitted over 1500 km for different $N_p$. The spectra are low-pass filtered as a result of transceiver and receiver bandwidth limitations. From the physical spectrum point of view, increasing $\alpha$ also comes with the expense of wider spectrum, with the 99%-energy bandwidth of 1-, 2- and 3-pass signals increased by 5%, 22% and 48% compared to conventional soliton signals with $\alpha = 0$ respectively. Nonetheless, the transmission reach improvement from Fig. 9 (c, d) for 2-pass signals is almost doubled for 16APSK and increased by 60% for 8PSK 2-pass signals. Therefore, the proposed scheme demonstrates a considerable improvement in the overall bandwidth-distance product of nonlinear transmission systems. Finally, it should be noted from Fig. 10 that the two classes of solitons with different eigenvalue real part will be more separated as $N_p$ increases and eventually approaches a conventional 2-channel WDM soliton system.

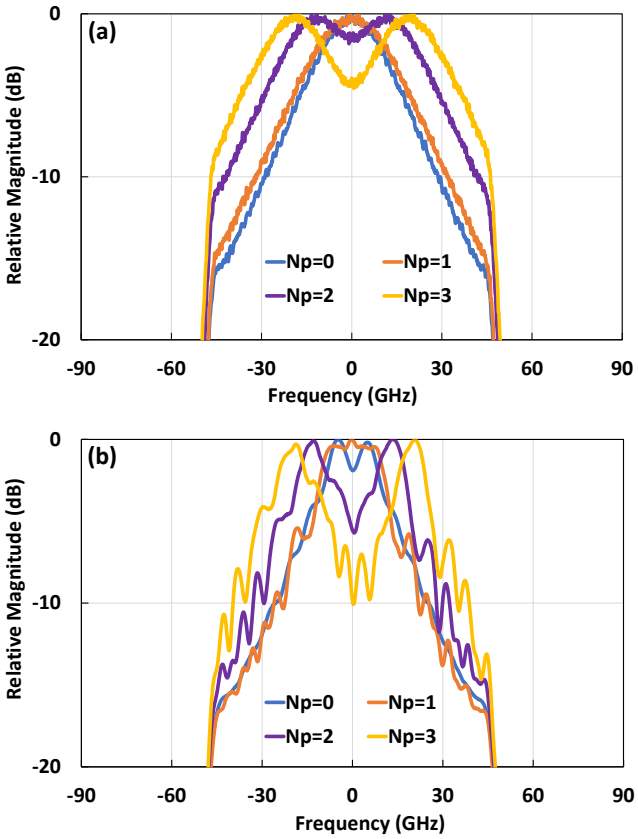


Fig. 10. (a) Back-to-back and (b) received spectrum for 6.13 Gbaud 8PSK signals transmitted over 1500 km with different pass-through number $N_p$. Increasing the real part of the eigenvalue $\alpha$ comes at the expense of broadened spectrum, but the overall bandwidth-distance product of the transmission system is improved.

## VI. Conclusions

In this paper, we theoretically and experimentally demonstrate that alternating the signs of the real part of eigenvalue $\alpha$ of neighboring solitons and allow them to collide and interact while the detection performance can be improved by choosing $\alpha$ such that the pulses are well separated at the receiver. The benefits of such interaction-tolerant design are experimentally demonstrated with 8PSK and 16APSK signals modulated on the $b$-coefficient where the transmission reach and bandwidth-distance product are significantly improved compared to conventional soliton transmissions. Our work illustrates how intentional soliton interactions can improve transmission performance. The results presented have only touched on the surface of several new dimensions for exploration such as multi-solitons, continuous spectrum, dual-polarization signal design as well as joint multi-pulse detection and signal processing, which will be investigated in the future.

## References


[1]. M. J. Ablowitz, and H. Segur, *Solitons and the inverse scattering transform*. Philadelphia, PA: SIAM, 1981.

[2]. L. F. Mollenauer, & J. P. Gordon, *Solitons in optical fibers: fundamentals and applications*, Academic Press, 2006.

[3]. J. P. Gordon, and H. A. Hermann. "Random walk of coherently amplified solitons in optical fiber transmission." Optics letters vol. 11, no. 10, pp. 665-667. Oct. 1986.

[4]. O. V. Yushko, A. A. Redyuk, M. P. Fedoruk, and S. K. Turitsyn. "Coherent soliton communication lines." *J. Exp. Theor. Phys.* vol. 119, no. 5, pp. 787-794, Nov. 2014.

[5]. O. V. Yushko, A. A. Redyuk, M. P. Fedoruk, K. J. Blow, N. J. Doran, A. D. Ellis, and S. K. Turitsyn. "Timing and phase jitter suppression in coherent soliton transmission." *Opt. Lett.* vol. 39, no. 21, pp. 6308-6311, Nov. 2014.

[6]. J. Satsuma, and Y. Nobuo. "B. Initial value problems of one-dimensional self-modulation of nonlinear waves in dispersive media," *Prog. Theor. Phys. Supp.*, vol. 55 np. 1, pp. 284-306, Jan. 1974.

[7]. J. P. Gordon, "Interaction forces among solitons in optical fibers." *Opt. Lett*, vol. 8, no. 11, pp. 596-598, Aug. 1983.

[8]. V. V. Afanasjev, and V. A. Vysloukh, "Interaction of initially overlapping solitons with different frequencies," JOSA B, vol. 11, no. 12, pp. 2385-2393, Dec. 1994.

[9]. V. I. Karpman, and V. V. Solov'eV. "A perturbational approach to the two-soliton systems." *Physica D.*, vol. 3, no. 3, pp. 487-502, Aug. 1981.

[10]. L. F. Mollenauer, S. G. Evangelides, and J. P. Gordon. "Wavelength division multiplexing with solitons in ultra-long distance transmission using lumped amplifiers." *J. Lightwave Technol.*, vol. 9 no. 3, pp. 362-367, Mar. 1991.

[11]. G. P. Agrawal, *Fiber-optic communication systems, 3rd edition.*, Hoboken, NJ, USA: Wiley, 2012.

[12]. E. Ip, and J. M. Kahn. "Compensation of dispersion and nonlinear impairments using digital backpropagation." *J. Lightwave Technol.*, Vol. 26 no. 20, pp. 3416-3425 OCT. 2008.

[13]. V. E. Zakharov and A. B. Shabat, "Exact theory of 2-dimensional selffocusing and one-dimensional self-modulation of waves in nonlinear media," *Sov. Phys. J. Exp. Theor. Phys*., vol. 34, no. 1, pp. 62–69, Jan. 1972.

[14]. A. Hasegawa and T. Nyu. "Eigenvalue communication." *J. Lightwave Technol.* vol. 11, no. 3, pp. 395-399, Mar. 1993.

[15]. E. G. Turitsyna and S. K. Turitsyn. "Digital signal processing based on inverse scattering transform, " *Opt. Lett*., vol. 38, no. 20, pp. 4186-4188, Oct. 2013.

[16]. M. I. Yousefi and F. R. Kschischang, "Information transmission using the nonlinear Fourier transform, Part I: mathematical tools," *IEEE Trans. Inf. Theory*, vol. 60, no. 7, pp. 4312–4328, Jul. 2014.

[17]. M. I. Yousefi and F. R. Kschischang, "Information transmission using the nonlinear Fourier transform, Part II: numerical methods," *IEEE Trans. Inf. Theory*, vol. 60, no. 7, pp. 4329–4345, Jul. 2014.

[18]. M. I. Yousefi and F. R. Kschischang, "Information transmission using the nonlinear Fourier transform, Part III: spectrum modulation," *IEEE Trans. Inf. Theory*, vol. 60, no. 7, pp. 4346–4369, Jul. 2014.

[19]. H. Bulow. "Experimental demonstration of optical signal detection using nonlinear Fourier transform." *J. Lightwave Technol.*, vol. 33, no. 7, pp. 1433-1439, Apr. 2015.

[20]. S. T. Le, J. E. Prilepsky, and S. K. Turitsyn. "Nonlinear inverse synthesis technique for optical links with lumped amplification." *Opt. express*, vol. 23, no. 7, pp. 8317-8328 Apr. 2015.

[21]. Z. Dong, S. Hari, T. Gui, K. Zhong, M. Yousefi, C. Lu, P-K. A. Wai, F. Kschischang, and A. P. T. Lau, "Nonlinear frequency division multiplexed transmissions based on NFT," *IEEE Photon. Technol. Lett.*, vol. 99, no. 15, pp. 1621-1623, Aug. 2015.

[22]. S. T. Le, V. Aref, and H. Buelow, "Nonlinear signal multiplexing for communication beyond the Kerr nonlinearity limit," *Nat. Photonics*, vol. 11 no. 9, pp. 570-576, Jul. 2017.

[23]. T. Gui, C. Lu, A. P. T. Lau, and P-K. A. Wai, "High-order modulation on a single discrete eigenvalue for optical communications based on nonlinear Fourier transform," *Opt. Express*, vol. 25, no. 17, pp. 20286-20297, Aug. 2017.

[24]. T. Gui, G. Zhou, C. Lu, A. P. T. Lau, and S. Wahls, "Nonlinear frequency division multiplexing with b-modulation: shifting the energy barrier," *Opt. Express*, vol. 26 no. 21, pp. 27978-27990 2018.

[25]. T. Gui, T. H. Chan, C. Lu, A. P. T. Lau, and P-K. A. Wai. "Alternative decoding methods for optical communications based on nonlinear Fourier transform," *J. Lightwave Technol*. vol. 35 no. 9, pp. 1542-1550, May 2017.

[26]. S. Gaiarin, A. M. Perego, E. P. da Silva, F. Da Ros, and D. Zibar. "Dual-polarization nonlinear Fourier transform-based optical communication system." *Optica*, vol. 5 no. 3, pp. 263-270, Mar. 2018.

[27]. W. A. Gemechu, T. Gui, J-W. Goossens, M. Song, S. Wabnitz, H. Hafermann, A. P. T. Lau, M. I. Yousefi, and Y. Jaouën. "Dual Polarization Nonlinear Frequency Division Multiplexing Transmission." *IEEE Photon. Technol. Lett*. vol. 30, no. 18, pp. 1589-1592, Sep. 2018.

[28]. X. Yangzhang, D. Lavery, P. Bayvel, and M. I. Yousefi. "Impact of Perturbations on Nonlinear Frequency-Division Multiplexing." *J. Lightwave Technol.*, vol. 36, no. 2, pp. 485-494, Jan. 2018.

[29]. V. Aref, H. Buelow, and K. Schuh. "On spectral phase estimation of noisy solitonic transmission." In *Optical Fiber Communication Conference*, California, Unite State, 2016, pp. W3A-3.

[30]. H. Buelow, V. Aref, and W. Idler. "Transmission of waveforms determined by 7 eigenvalues with PSK-modulated spectral amplitudes." In *European Conference on Optical Communication*, Dusseldorf, German, 2016, pp. 1-3. VDE.

[31]. R. T. Jones, S. Gaiarin, M. P. Yankov, and D. Zibar. "Time-Domain Neural Network Receiver for Nonlinear Frequency Division Multiplexed Systems." *IEEE Photon. Technol. Lett.*, vol. 30, no. 12, pp. 1079-1082, Apr. 2018.

[32]. M. K. Kopae, J. E. Prilepsky, S. T. Le, and S. K. Turitsyn. "Optical communication based on the periodic nonlinear Fourier transform signal processing." In *International Conference on Photonics*, Kuching, Malaysia, 2016, pp. 1-3.

[33]. L. L. Frumin., A. A. Gelash, and S. K. Turitsyn. "New approaches to coding information using inverse scattering transform." *Phys. Rev. lett.*, vol. 118, no. 22, pp. 223901, Jun. 2017.

[34]. S. Hari, and F. R. Kschischang, "Bi-directional algorithm for computing discrete spectral amplitudes in the NFT," *J. Lightvave Technol*., vol. 34, no. 15, pp. 3529-3537, Aug. 2016.

[35]. S. Wahls, and H. V. Poor. "Fast numerical nonlinear Fourier transforms," *IEEE Trans. Inf. Theory*, vol. 61, no. 12, pp. 6957-6974, Dec. 2015.

[36]. V. Aref, "Control and detection of discrete spectral amplitudes in nonlinear Fourier spectrum." *arXiv preprint arXiv:1605.06328* (2016).

[37]. S. Wahls, and H. V. Poor. "Fast inverse nonlinear Fourier transform for generating multi-solitons in optical fiber," in *International Symposium on Information Theory (ISIT)*, Hong Kong, China, 2015, pp. 1676-1680.

[38]. L. L. Frumin, O. V. Belai, E. V. Podivilov, and D. A. Shapiro, "Efficient numerical method for solving the direct Zakharov–Shabat scattering problem," *JOSA B*, vol. 32, no. 2, pp. 290-296, Feb. 2015.

[39]. J. E. Prilepsky, S. A. Derevyanko, and S. K. Turitsyn. "Temporal solitonic crystals and non-Hermitian informational lattices." *Phys. Rev. Lett.*, vol. 108, no. 18, pp. 183902, May 2012.

[40]. G. P. Agrawal, *Nonlinear fiber optics*. San Diego, CA, USA: Academic Press, 2007.

[41]. S. Civelli, E. Forestieri, and M. Secondini, "Impact of discretization and boundary conditions in nonlinear frequency-division multiplexing," In *Proc. 18th Italian Nat. Conf. Photon. Technol.*, 2016, pp. 1–4.

[42] I. T. Lima, T. D. S. DeMenezes, V. S. Grigoryan, M. O'Sullivan, and C. R. Menyuk, "Nonlinear compensation in optical communications systems with normal dispersion fibers using the nonlinear Fourier transform," *J. Lightw. Technol*., vol. 35, no. 23, pp. 5056–5068, 2017.

[43] I. T. Lima, V. S. Grigoryan, M. O'Sullivan and C. R. Menyuk. "Computational complexity of nonlinear transforms applied to optical communications systems with normal dispersion fibers." In *Proc. IEEE Photo. Conf.*, Reston, VA, USA, Oct. 2015, vol. 3, pp. 277–278.

[44]. Q. Zhang, and T. H. Chan. "A Gaussian noise model of spectral amplitudes in soliton communication systems." In *IEEE 16th International Workshop on Signal Processing Advances in Wireless Communications (SPAWC)*, Stockholm, Sweden, 2015, pp. 455-459.

[45]. V. Aref, "Nonlinear Fourier Transform of Truncated Multi-Soliton Pulses." In *12th International ITG Conference on Systems, Communications and Coding*, Rostock, German, 2019, p. 1-6, VDE.

[46]. A. Span, V. Aref, H. Bülow, and S. T. Brink. "On time-bandwidth product of multi-soliton pulses." In *2017 IEEE International Symposium on Information Theory (ISIT)*, Aachen, Germany, pp. 61-65. 2017.

[47]. S. T. Le, and H. Buelow. "Nonlinear frequency division multiplexed transmissions with 64QAM." In *Opto-Electronics and Communications Conference (OECC) and Photonics Global Conference (PGC)*, Singapore, 2017, pp. 1-2.

[48]. A. Alvarado, E. Agrell, D. Lavery, R. Maher, and P. Bayvel. "Replacing the soft-decision FEC limit paradigm in the design of optical communication systems". *J. Lightwave Technol*., vol. 33, no. 20, pp. 4338-4352, OCT. 2015.